



You have downloaded a document from
RE-BUŚ
repository of the University of Silesia in Katowice

Title: Analysis of normal human retinal vascular network architecture using multifractal geometry

Author: Ștefan Țălu, Sebastian Stach, Dan Mihai Călugăru, Carmen Alina Lupașcu, Simona Delia Nicoară

Citation style: Țălu Ștefan, Stach Sebastian, Călugăru Dan Mihai, Lupașcu Carmen Alina, Nicoară Simona Delia. (2017). Analysis of normal human retinal vascular network architecture using multifractal geometry. "International Journal of Ophthalmology" (2017, Vol. 10, Iss. 3, s. 434-438), doi 10.18240/iio.2017.03.17



Uznanie autorstwa - Użycie niekomercyjne - Bez utworów zależnych Polska - Licencja ta zezwala na rozpowszechnianie, przedstawianie i wykonywanie utworu jedynie w celach niekomercyjnych oraz pod warunkiem zachowania go w oryginalnej postaci (nie tworzenia utworów zależnych).



UNIwersYTET ŚLĄSKI
W KATOWICACH



Biblioteka
Uniwersytetu Śląskiego



Ministerstwo Nauki
i Szkolnictwa Wyższego

Analysis of normal human retinal vascular network architecture using multifractal geometry

Ștefan Țălu¹, Sebastian Stach², Dan Mihai Călugăru³, Carmen Alina Lupașcu⁴, Simona Delia Nicoară³

¹Discipline of Descriptive Geometry and Engineering Graphics, Department of AET, Faculty of Mechanical Engineering, Technical University of Cluj-Napoca, 103-105 B-dul Muncii St., Cluj-Napoca 400641, Cluj, Romania

²Department of Biomedical Computer Systems, Institute of Informatics, Faculty of Computer Science and Materials Science, University of Silesia, Będzińska 39, 41-205 Sosnowiec, Poland

³Discipline of Ophthalmology, Department of Surgical Specialties and Medical Imaging, Faculty of Medicine, "Iuliu Hațieganu" University of Medicine and Pharmacy Cluj-Napoca, 8 Victor Babeș St., Cluj-Napoca 400012, Cluj, Romania

⁴Department of Mathematics and Informatics, University of Palermo, Via Archirafi 34, Palermo 90123, Italy

Correspondence to: Ștefan Țălu. Discipline of Descriptive Geometry and Engineering Graphics, Department of AET, Faculty of Mechanical Engineering, Technical University of Cluj-Napoca, 103-105 B-dul Muncii St., Cluj-Napoca 400641, Cluj, Romania. stefan_ta@yahoo.com

Received: 2015-12-16 Accepted: 2016-08-18

Abstract

• **AIM:** To apply the multifractal analysis method as a quantitative approach to a comprehensive description of the microvascular network architecture of the normal human retina.

• **METHODS:** Fifty volunteers were enrolled in this study in the Ophthalmological Clinic of Cluj-Napoca, Romania, between January 2012 and January 2014. A set of 100 segmented and skeletonised human retinal images, corresponding to normal states of the retina were studied. An automatic unsupervised method for retinal vessel segmentation was applied before multifractal analysis. The multifractal analysis of digital retinal images was made with computer algorithms, applying the standard box-counting method. Statistical analyses were performed using the GraphPad InStat software.

• **RESULTS:** The architecture of normal human retinal microvascular network was able to be described using the multifractal geometry. The average of generalized dimensions (D_q) for $q=0, 1, 2$, the width of the multifractal spectrum ($\Delta\alpha=\alpha_{max} - \alpha_{min}$) and the spectrum arms' heights difference ($|\Delta f|$) of the normal images were expressed as mean±standard deviation (SD): for segmented versions,

$D_0=1.7014\pm 0.0057$; $D_1=1.6507\pm 0.0058$; $D_2=1.5772\pm 0.0059$; $\Delta\alpha=0.92441\pm 0.0085$; $|\Delta f|=0.1453\pm 0.0051$; for skeletonised versions, $D_0=1.6303\pm 0.0051$; $D_1=1.6012\pm 0.0059$; $D_2=1.5531\pm 0.0058$; $\Delta\alpha=0.65032\pm 0.0162$; $|\Delta f|=0.0238\pm 0.0161$. The average of generalized dimensions (D_q) for $q=0, 1, 2$, the width of the multifractal spectrum ($\Delta\alpha$) and the spectrum arms' heights difference ($|\Delta f|$) of the segmented versions was slightly greater than the skeletonised versions.

• **CONCLUSION:** The multifractal analysis of fundus photographs may be used as a quantitative parameter for the evaluation of the complex three-dimensional structure of the retinal microvasculature as a potential marker for early detection of topological changes associated with retinal diseases.

• **KEYWORDS:** generalized dimensions; multifractal; retinal vessel segmentation; retinal image analysis; retinal microvasculature; standard box-counting method

DOI:10.18240/ijo.2017.03.17

Țălu Ș, Stach S, Călugăru DM, Lupașcu CA, Nicoară SD. Analysis of normal human retinal vascular network architecture using multifractal geometry. *Int J Ophthalmol* 2017;10(3):434-438

INTRODUCTION

The human retinal vascular imaging, as a noninvasive research tool, can provide precise quantification of subtle retinal vascular changes associated with retinal vascular diseases^[1-3].

The human retinal microvasculature is the only microcirculation with a complex topological architecture that can be observed *in vivo* using a retinal camera and can provide potentially valuable disease biomarkers^[3-5].

Over the last few decades, the human retinal microvascular network is especially relevant to modern ophthalmology because it has the potential to reveal important information for detection and quantify the retinal systemic vascular diseases^[1,5-7] and non-vascular pathology^[8-10]. Previous studies have established that the ocular vascular diseases modify the three-dimensional morphology of retinal blood vessels and the optimal density for capillary networks^[2,7,9].

The analysis of the relationship between the changes in retinal blood vessel topological parameters and retinal diseases, using different computerized methods, is used to detect and treatment of the retinal diseases in the early stages^[2-3,5].

The natural morphological complexity of the eye is a major factor contributing to the limits of the application of Euclidean geometry to the study of the complex architecture of the human retinal microvasculature^[7,11-13].

Digital retinal photographs of the complex patterns structures of the human retinal microvasculature that can not be described and measured properly in a correct manner using Euclidean geometry can be characterized using fractal^[8,11-12,14-22] and multifractal geometry^[13,23-26].

In ophthalmology, the fractal and multifractal geometries offer a mathematical approach for the quantification of the human retinal microvasculature, over a range of spatial, temporal, and organizational scales^[7,14,22-24].

Previous reports indicated that the mechanisms and factors implied in the development of human retinal microvasculature, both normal and pathological, owing to their complex hierarchical organization, are not fully understood and need to be researched further^[7-8,14].

The three-dimensional human retinal microvascular network can be analyzed and estimated if it is considered as fractal or multifractal object in a "scaling window", which normally ranges in two to three orders of magnitude^[27].

Fractal analysis describes the global measurement of complexity of the human retinal vessel branching, which is expressed by the mean fractal dimension (D) value (a valid estimator with a fractional value)^[7,14,19,22].

In several fractal analysis studies of the normal human retinal microvascular network, determined by box-counting method, the mean fractal dimension (D) value was approximately 1.7^[15,17-19].

Some reports indicated that human retinal microvascular network has a multifractal geometrical structure^[23-26].

Multifractal analysis provides us a deep insight into the complex nature of spatial distribution and geometry (a description over the retinal regions both locally and globally)^[23-26].

In many studies, researchers have found different fractal dimensions D ^[14,17-20] or generalized dimensions D_q (for $q=0, 1, 2$) values^[23-26] associated with normal human retinal microvascular network and their results sometimes reveal discordances because of differences in the experimental and methodological parameters involved.

The fractal and multifractal analyses of retinal vascular network depend on the fractal analysis methods, multifractal methods, including the algorithm and specific calculation used *etc*^[7,23,28-31].

MATERIALS AND METHODS

Multifractal Analysis In our study the multiple scalings are analyzed through multifractal spectrum.

The common multifractal measures are: 1) the generalized fractal dimensions function D_q , where q is a real parameter that indicates the order of the moment of the measure; 2) the $f(\alpha)$

singularity spectrum, where α is named Hölder or singularity exponent^[23-25]. There are some mathematical methods to compute this spectrum, according references^[23-25].

The generalized dimensions D_q for $q=0, 1$ and 2 , are known as the capacity (or box-counting), the information and correlation dimensions, respectively. The capacity dimension D_0 is independent of q and provides global (or average) information about the structure, D_1 quantifies the degree of disorder present in the distribution, and D_2 measures the mean distribution density of the statistical measure^[25]. All dimensions are different, satisfying $D_0 > D_1 > D_2$.

The retinal microvascular network can be associated with a multifractal structure if there is a statistically significant difference between D_0, D_1 and D_2 ^[23-25].

Segmentation Method The segmentation consists of extracting geometric information about the retinal vessels from the eye fundus images. The quality of the segmentation is quite dependent on the parameters used such as image quality, choice of threshold, and choice of structuring elements^[31-35]. The color images were converted in a binary format.

In this study, an automatic unsupervised method for the segmentation of retinal vessels^[32] was applied before multifractal analysis, according to the segmentation methodology and computer algorithms proposed in reference^[33-35].

Materials This study was conducted according to the Declaration of Helsinki and the European Guidelines on Good Clinical Practice for research in human subjects.

All adult volunteers were provided with written informed consent prior to enrollment in the study. The approval of the Ethics Committee of "Iuliu Hațieganu" University of Medicine and Pharmacy Cluj-Napoca, Romania, was obtained.

Normal healthy adult subjects consisted of 50 volunteers (male gender, 52%; age, 49±6.1y) with normal posterior Pole, without ocular or systemic diseases and no current smoking history participated in this study from January 2012 to January 2014. All participants underwent a standardized interview, including a medical history review, and ocular and systemic examination.

After maximal pharmacologic pupil dilation, retinal images centered on the macula and optic disc of each eye, available for retinal vascular analysis, were captured digitally using a fundus camera at 45° field of view (VISUCAM^{Lite} Zeiss; Carl Zeiss Meditec AG 07740 Jena 2008, Germany). Digital retinal photographs were taken of both eyes. Each subject was examined in a room at (24 °C ±1 °C), with standard indoor levels of illumination (300 lx) and humidity (50%±1%), and no air drafts.

A set of 100 segmented and skeletonised human retinal images, corresponding to normal states of the retina has been studied. The results were expressed as mean±standard deviation (SD).

Methods The multifractal analyses were made according to the multifractal methodology proposed in reference^[23]. An analysis of the digital retinal files was conducted based on the original algorithm (in MATLAB software R2012b, MathWorks, Inc.)^[36]. This is derived directly from the definition of the box-counting fractal dimension^[37].

Multifractal analysis was performed, for the entire retinal image, applying the standard box-counting algorithm to the digitized data, in two cases: 1) on the segmented images (seg.); 2) on the skeletonised (skl.) version.

The $f(\alpha)$ spectrum was computed in the range $-10 \leq q \leq 10$ for successive 1.0 steps.

After adjustments of every digital image, the segmented version of retinal vessel structure contains the vessel silhouettes extracted from the fundus photographs.

The vessel maps (8-bit) were then skeletonised. This procedure was applied for all analyzed structures and all the skeletonised images were obtained with the Image J skeletonising algorithm^[38].

Statistical Analysis The statistical processing of the results (Table 1) was done using GraphPad InStat software program, version 5.00^[39]. A value of $P < 0.05$ was regarded as being statistically significant. The average results were expressed as mean value and SD.

RESULTS

Results of Multifractal Analysis A summary of the obtained results of the generalized dimensions (D_q) for $q=0, 1, 2$, the width of the multifractal spectrum ($\Delta\alpha = \alpha_{max} - \alpha_{min}$) and the spectrum arms' heights difference ($| \Delta f |$), all with average \pm SD, of 100 analyzed images, for normal (N) status, in segmented and skeletonised variants, is presented in the Table 1. Figures 1-4 show the results of multifractal analyses, plots of $\alpha(q, r)$ versus q , $f(q, r)$ versus q and of $f(q, r)$ versus $\alpha(q, r)$, for normal retinal vessel network (Figure 5A), in segmented (seg.) and skeletonised (skl.) variants (where r is box size in the given scale).

$| \Delta f | = f_{max} - f_{min}$, when $f(\alpha) > 0$, represents the spectrum arms' heights difference.

DISCUSSION

Improvements in digital retinal imaging have led to quantification of the complex three-dimensional structure of the normal human retinal microvasculature network. Our findings confirm that normal human retinal microvascular network can be described and estimated using the multifractal geometry.

The average of generalized dimensions (D_q) for $q=0, 1, 2$, the width of the multifractal spectrum ($\Delta\alpha = \alpha_{max} - \alpha_{min}$) and the spectrum arms' heights difference ($| \Delta f |$), of the normal images were expressed as mean \pm SD: 1) for segmented versions, $D_0 = 1.7014 \pm 0.0057$; $D_1 = 1.6507 \pm 0.0058$; $D_2 = 1.5772 \pm 0.0059$; $\Delta\alpha = 0.92441 \pm 0.0085$; $| \Delta f | = 0.1453 \pm 0.0051$; 2) for skeletonised versions, $D_0 = 1.6303 \pm 0.0051$; $D_1 = 1.6012 \pm 0.0059$; $D_2 = 1.5531 \pm 0.0058$; $\Delta\alpha = 0.65032 \pm 0.0162$; $| \Delta f | = 0.0238 \pm 0.0161$.

Table 1 The generalized dimensions (D_q) for $q=0, 1, 2$, the width of the multifractal spectrum ($\Delta\alpha = \alpha_{max} - \alpha_{min}$) and the spectrum arms' heights difference ($| \Delta f |$), all with average \pm SD, of 100 analyzed images, for normal (N) status, in segmented and skeletonised variants

| Status (N) | Segmented | Skeletonised | P |
|--|----------------------|----------------------|-------|
| D_0 | 1.7014 \pm 0.0057 | 1.6303 \pm 0.0051 | 0.035 |
| D_1 | 1.6507 \pm 0.0058 | 1.6012 \pm 0.0059 | 0.038 |
| D_2 | 1.5772 \pm 0.0059 | 1.5531 \pm 0.0058 | 0.032 |
| $\Delta\alpha = (\alpha_{max} - \alpha_{min})$ | 0.92441 \pm 0.0085 | 0.65032 \pm 0.0162 | 0.029 |
| $ \Delta f = f_{max} - f_{min}$ | 0.1453 \pm 0.0051 | 0.0238 \pm 0.0161 | 0.033 |

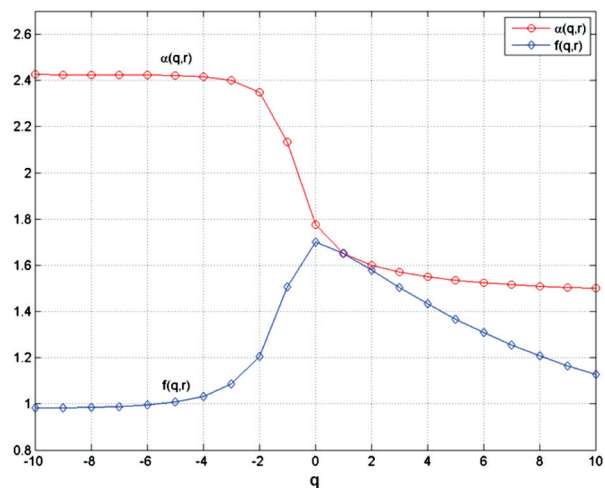


Figure 1 Plot of $\alpha(q, r)$ versus q and of $f(q, r)$ versus q , in segmented variant The $\alpha(q, r)$ curve decreases from 2.4254 (for $q = -10$) and tends to 1.5009 (for $q = 10$). The $f(q, r)$ curve increases from $q = 0.9816$ (for $q = -10$) to a maximum value of 1.7015 (for $q = 0$), then decreases and tends to 1.1269 for $q = 10$.

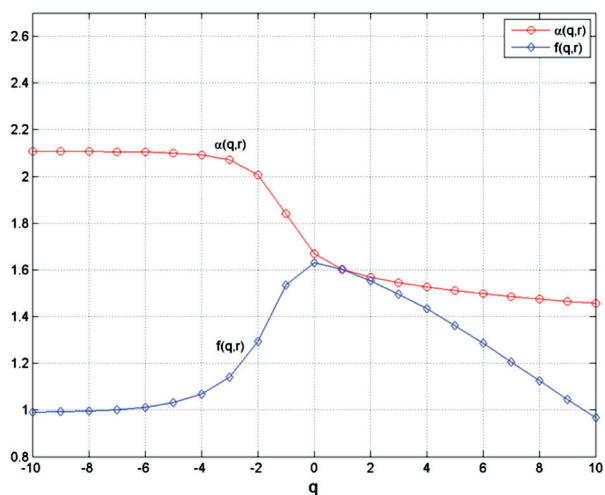


Figure 2 Plot of $\alpha(q, r)$ versus q and of $f(q, r)$ versus q , in skeletonised variant The $\alpha(q, r)$ curve decreases from 2.1072 (for $q = -10$) and tends to 1.4569 (for $q = 10$). The $f(q, r)$ curve increases from $q = 0.9910$ (for $q = -10$) to a maximum value of 1.6306 (for $q = 0$), then decreases and tends to 0.9672 for $q = 10$.

The average of generalized dimensions (D_q) for $q=0, 1, 2$, the width of the multifractal spectrum ($\Delta\alpha$) and the spectrum arms' heights difference ($| \Delta f |$) of the segmented versions are slightly greater than the skeletonised versions. This study confirms the obtained results in previous multifractal studies shown in reference^[24].

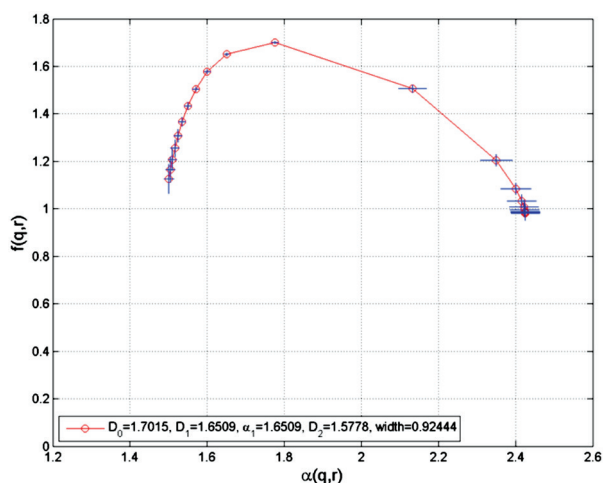


Figure 3 Plot of $f(q, r)$ versus $\alpha(q, r)$ in segmented variant The left branch of the spectrum corresponds to large q values ($q > 0$), while the right branch of the spectrum corresponds to small q values ($q < 0$). The $f(q, r)$ curve has a maximum value of 1.7015 corresponding to $q = 0$.

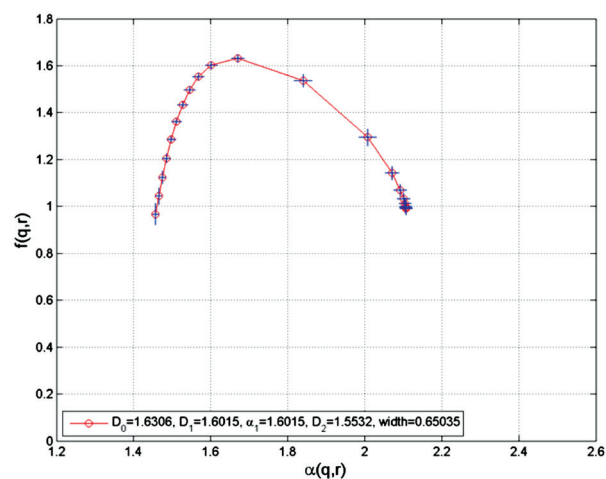


Figure 4 Plot of $f(q, r)$ versus $\alpha(q, r)$ in skeletonised variant The left branch of the spectrum corresponds to large q values ($q > 0$), while the right branch of the spectrum corresponds to small q values ($q < 0$). The $f(q, r)$ curve has a maximum value of 1.6306 corresponding to $q = 0$.

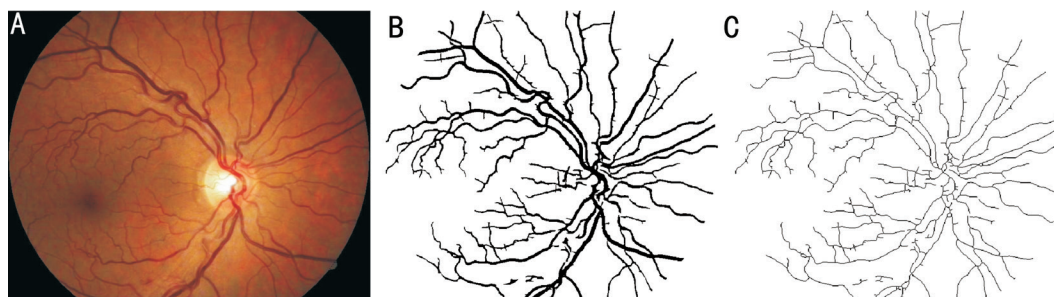


Figure 5 Images of the retina vessel network for a normal subject A: Original color; B: Segmented (seg.); C: Skeletonised (skl.) variants. The optic disc is the brightest region having elliptical shape which appears bright orange pink with a pale center. The retinal vessels coming from the optic disc have a normal branching pattern.

In conclusion, the non-Euclidean three-dimensional nature of human retina microvascular network across the physiopathological spectrum can be analyzed and quantified using the multifractal geometry.

The graphs in Figures 1-4 demonstrate the multifractal geometrical organization of the normal human retina microvascular network, that is not evident in the fractal dimensions. A benefit of the proposed multifractal methodology is the elegance of the algorithm, computational effectiveness and its interpretation.

The multifractal analysis of fundus photographs (with all the intrinsic limitations as a mathematical model) may be used as an objective and quantitative parameter for the evaluation of the human retina microvascular network. It is reasonable to assume that its identification as a potential marker for early detection of topological changes associated with retinal diseases will help investigators to design specific retinal treatment strategies.

ACKNOWLEDGEMENTS

This paper was performed within the frame of the Program "Partnerships in priority domains" with the support of the National Education Ministry, the Executive Agency for Higher Education, Research, Development and Innovation

Funding (UEFISCDI), Romania (Project code: PN-II-PT-PC-CA-2013-4-1232).

Conflicts of Interest: Țălu Ș, None; Stach S, None; Călugăru DM, None; Lupașcu CA, None; Nicoară SD, None.

REFERENCES

- 1 Parsons-Wingterter P, Radhakrishnan K, Vickerman MB, Kaiser PK. Oscillation of angiogenesis with vascular dropout in diabetic retinopathy by VESSEL GENERATION analysis (VESGEN). *Invest Ophthalm Vis Sci* 2010; 51(1):498-507.
- 2 Țălu SD. *Ophthalmologie:Cours*. Medical publishing house "Iuliu Hațieganu", Cluj-Napoca, Romania, 2005.
- 3 Călugăru M, Călugăru D. *Ophthalmology*. Publishing house Toderco, Cluj-Napoca, Romania, 2004.
- 4 Țălu S. Mathematical models of human retina. *Oftalmologia* 2011; 55(3):74-81.
- 5 Nirmala SR, Nath MK, Dandapat S. Retinal image analysis: a review. *International Journal of Computer and Communication Technology* 2011; 2(6):11-14.
- 6 Țălu Ș, Țălu M, Giovanzana S, Shah R. The history and use of optical coherence tomography in ophthalmology. *HVM Bioflux* 2011;3(1):29-32. <http://www.hvm.bioflux.com.ro/docs/2011.3.29-32.pdf>
- 7 Țălu Ș. Characterization of retinal vessel networks in human retinal imagery using quantitative descriptors. *HVM Bioflux* 2013;5(2):52-57.

- 8 Liew G, Wang JJ, Cheung N, Zhang YP, Hsu W, Lee ML, Mitchell P, Tikellis G, Taylor B, Wong TY. The retinal vasculature as a fractal: methodology, reliability, and relationship to blood pressure. *Ophthalmology* 2008;115(11):1951-1956.
- 9 Heringa SM, Bouvy WH, van den Berg E, Moll AC, Kappelle LJ, Biesseles GJ. Associations between retinal microvascular changes and dementia, cognitive functioning, and brain imaging abnormalities: a systematic review. *J Cereb Blood Flow Metab* 2013;33(7):983-995.
- 10 Lim LS, Cheung CY, Sabanayagam C, Lim SC, Tai ES, Huang L, Wong TY. Structural changes in the retinal microvasculature and renal function. *Invest Ophthalmol Vis Sci* 2013;54(4):2970-2976.
- 11 Szabo B, Țălu Ș, Lupașcu CA. Application of fractal dimension in analysis of human retinal images in malignant choroidal melanoma patients. *Sylvan Journal* 2014;158(7):1-10.
- 12 Țălu Ș, Călugăru DM, Lupașcu CA. Characterisation of human non-proliferative diabetic retinopathy using the fractal analysis. *Int J Ophthalmol* 2015;8(4):770-776.
- 13 Țălu Ș, Vlăduțiu C, Lupașcu CA. Characterization of human retinal vessel arborisation in normal and amblyopic eyes using multifractal analysis. *Int J Ophthalmol* 2015;8(5):996-1002.
- 14 Kyriacos S, Nekka F, Vicco P, Cartilier L. The retinal vasculature: towards an understanding of the formation process. In: Vehel LJ, Lutton E, Tricot G (Eds.). *Fractals in engineering-from theory to industrial applications*. Germany: Springer; 1997;383-397.
- 15 Țălu Ș. The influence of the retinal blood vessels segmentation algorithm on the monofractal dimension. *Oftalmologia* 2012;56(3):73-83.
- 16 Grauslund J, Green A, Kawasaki R, Hodgson L, Sjolie AK, Wong TY. Retinal vascular fractals and microvascular and macrovascular complications in type 1 diabetes. *Ophthalmology* 2010;117(7):1400-1405.
- 17 Țălu Ș, Giovanzana S. Fractal and multifractal analysis of human retinal vascular network: a review. *HVM Bioflux* 2011;3(3):205-212.
- 18 Țălu Ș. Fractal analysis of normal retinal vascular network. *Oftalmologia* 2011;55(4):11-16.
- 19 Țălu Ș, Giovanzana S. Image analysis of the normal human retinal vasculature using fractal geometry. *HVM Bioflux* 2012;4(1):14-18.
- 20 Azemin MZ, Kumar DK, Wong TY, Wang JJ, Mitchell P, Kawasaki R, Wu H. Age-related rarefaction in the fractal dimension of retinal vessel. *Neurobiol Aging* 2012;33(1):194-191.
- 21 Țălu Ș, Vlăduțiu C, Popescu LA, Lupașcu CA, Vesa ȘC, Țălu SD. Fractal and lacunarity analysis of human retinal vessel arborisation in normal and amblyopic eyes. *HVM Bioflux* 2013;5(2):45-51. <http://www.hvm.bioflux.com.ro/docs/2013.45-51.pdf>
- 22 MacGillivray TJ, Patton N, Doubal FN, Graham C, Wardlaw JM. Fractal analysis of the retinal vascular network in fundus images. *Conf Proc IEEE Eng Med Biol Soc* 2007;2007:6456-6459.
- 23 Stosic T, Stosic B. Multifractal analysis of human retinal vessels. *IEEE Trans Med Imaging* 2006;25(8):1101-1107.
- 24 Țălu Ș. Multifractal characterisation of human retinal blood vessels. *Oftalmologia* 2012;56(2):63-71.
- 25 Țălu Ș. Multifractal geometry in analysis and processing of digital retinal photographs for early diagnosis of human diabetic macular edema. *Curr Eye Res* 2013; 38(7):781-792.
- 26 Țălu Ș, Fazekas Z, Țălu M, Giovanzana S. Analysis of human peripapillary atrophy using computerised image analysis. In: The 9th Conference of the Hungarian Association for Image Processing and Pattern Recognition (KÉPAF 2013), 29 January-1 February 2013, Bakonybél, Hungary, 427-438. http://kepaf2013.mik.uni-pannon.hu/proceedings/pdfs/F08_04.pdf
- 27 Losa GA, Merlini D, Nonnenmacher TF, Weibel E (Eds.). *Fractals in biology and medicine. Vol. IV. Mathematics and bioscience in interaction*. Basel, Switzerland; Birkhäuser Verlag; 2005.
- 28 Khan MI, Shaikh H, Mansuri AM, Soni P. A review of retinal vessel segmentation techniques and algorithms. *International Journal of Computer Technology and Applications* 2011;2(5):1140-1144.
- 29 Țălu Ș. Mathematical methods used in monofractal and multifractal analysis for the processing of biological and medical data and images. *Anim Biol Anim Husb* 2012;4(1):1-4.
- 30 Țălu Ș. Texture analysis methods for the characterisation of biological and medical images. *Extreme Life, Biospeology & Astrobiology* 2012; 4(1):8-12. <http://www.elba.bioflux.com.ro/docs/2012.4.8-13.pdf>
- 31 Fraz MM, Remagnino P, Hoppe A, Uyyanonvara B, Rudnicka AR, Owen CG, Barman SA. Blood vessel segmentation methodologies in retinal images-a survey. *Computer Methods Programs Biomed* 2012;108(1):407-333.
- 32 Lupașcu CA, Tegolo D. *Stable automatic unsupervised segmentation of retinal vessels using self-organizing maps and a modified fuzzy C-means clustering*. Proc. of WILF 2011, Trani, Italy, 2011;244-252, Lecture Notes in Artificial Intelligence (LNAI 6857), Subseries of Lecture Notes in Computer Science (LNCS), Springer-Verlag Berlin Heidelberg 2011.
- 33 Lupașcu CA, Tegolo D, Trucco E. FABC: Retinal vessel segmentation using AdaBoost. *IEEE Trans Inf Technol Biomed* 2010;14(5):1267-1274.
- 34 Lupașcu CA, Tegolo D. *Automatic unsupervised segmentation of retinal vessels using self-organizing maps and K-means clustering*. Proc. of CIBB 2010, Palermo, Italy, 2010;263-274, Lecture Notes in Bioinformatics (LNBI 6685), Subseries of Lecture Notes in Computer Science (LNCS), Springer-Verlag Berlin Heidelberg 2011;(6685):263-274.
- 35 Lupașcu CA, Tegolo D, Trucco E. *A comparative study on feature selection for retinal vessel segmentation using FABC*. Proc. of CAIP 2009, Münster, Germany, 2009;655-662, Lecture Notes in Computer Science (LNCS) 5702, Springer-Verlag Berlin Heidelberg 2009;655-662.
- 36 Stach S, Roskosz S, Cybo J, Cwajna J. Properties of sialon ceramics evaluated by means of multifractal, surface stereometry and quantitative fractography techniques. *Mater Charact* 2009;60(10):1151-1157.
- 37 Țălu Ș. *Micro and nanoscale characterization of three dimensional surfaces. Basics and applications*. Napoca Star Publishing House, Cluj-Napoca, Romania 2015. ISBN 978-606-690-349-3.
- 38 Image J software, version ImageJ 1.48g (Wayne Rasband, National Institutes of Health, Bethesda, Maryland, USA). Available from: <http://imagej.nih.gov/ij>. Accessed on July 10th, 2016.
- 39 GraphPad InStat software, version 5.00 (GraphPad, San Diego, California, USA). Available from: <http://www.graphpad.com/instat/instat.htm>. Accessed on July 10th, 2016.